Workshop on Stellar Dynamos
ASP Conference Series, Vol. 178, 1999
M. Núñez, A. Ferriz-Mas (eds.)

Simulations and observations of stellar dynamos: evidence for a magnetic alpha-effect

Axel Brandenburg

Department of Mathematics, University of Newcastle upon Tyne, NE1 7RU, UK

Abstract. There are now several simulations showing the generation of large scale magnetic fields whose energy exceeds the kinetic energy of the turbulence. Those simulations have in common that the large scale field generation is related to some kind of a magnetic instability (magnetorotational instability, magnetic buoyancy instability and in some cases even the kink instability). The large scale field generation sets in after some level of small scale dynamo activity has been established, suggesting that the large scale field generation is essentially nonkinematic. This mechanism is also essentially anisotropic, because the various instabilities mentioned above do not exist under isotropic conditions (shear, rotation and gravity are needed). Some aspects of the field generation are reproduced by α-effect dynamos, which can be compared with observations.

1. Dynamos from overshooting convection with shear

The overshoot layer beneath the solar convection zone proper is often thought to be the place where the dynamo operates. This is the main reason why it is useful to include overshoot in convective dynamo simulations. Results of Nordlund et al. (1992) and Brandenburg et al. (1996) suggest that dynamo action occurs actually throughout the entire convection zone proper, but that the field is then transported downwards into the overshoot layer by turbulent pumping of magnetic fields via rapidly spinning downdrafts. Recently, those simulations have been extended to include the effects of shear (Brandenburg et al. 1999). Shear takes the role of the omega-effect, although here the concept of alpha-omega dynamos is not explicitly invoked. The main result is the generation of large scale fields on the scale of the box. Those fields are of significant strength and can exceed the equipartion field strength by an order of magnitude.

For orientation we give the basic parameters of the simulation. The simulation is carried out at 30° northern latitude and the resulting inverse Rossby number, $2\Omega L/u_{\rm rms}$, is around 5. Here, $u_{\rm rms}$ is the turbulent rms velocity, L is the depth of the unstable layer, and Ω is the angular velocity. Uniform latitudinal shear is imposed by a body force throughout the convection zone proper, but it vanishes towards the radiative interior, resulting in vertical shear

around the lower overshoot layer. 'Sliding-periodic' boundary conditions (Hawley et al. 1995) are used in the cross-stream direction and ordinary periodic boundary conditions in the streamwise direction. The ratio between shear gradient and angular velocity is 0.5 and the velocity difference across the box is $\Delta U \approx \pm 0.4 u_{\rm rms}$. The resolution is $63 \times 63 \times 64$ meshpoints, the ordinary and magnetic Prandtl numbers are ${\rm Pr} = \nu/\chi = 0.2$ and ${\rm Pr}_M = \nu/\eta = 0.5$, i.e. the kinematic viscosity ν is smaller than the magnetic and thermal diffusivities (η and χ). In the sun the two Prandtl numbers are much smaller than unity, but this is impossible to simulate in a simulation of only modest resolution. The Reynolds number is ${\rm Re} = u_{\rm rms} L/\nu = 240$, the Rayleigh and Taylor numbers are ${\rm Ra} = g L^4 s_0'/(c_p \chi \nu) = 5 \times 10^5$ and ${\rm Ta} = (2\Omega L^2/\nu) = 10^6$. Here, g is gravity and s_0' is the entropy gradient of the associated unstable hydrostatic solution.

The orientation of the cartesian box is as follows: x points north, y points east in the toroidal direction, and z points downwards. The top and bottom boundaries are stress free and the horizontal field vanishes, so there is no vertical Poynting flux through the boundaries. Initially there is no net flux through the box.

In figure 1 we show the evolution of the total magnetic energy and the mean magnetic field in such a simulation. The magnetic energy increases by 6 orders of magnitude and then saturates. There is also an exponential growth of the *mean* field (averaged over the entire box), which increases by 3 orders of magnitude until saturation is reached. (This is at around $t = 3200$, approximately the same time when the magnetic energy saturates; the time unit is $\sqrt{L/g}$.) Note that the energy in the mean magnetic field can be as large as 20% of the total magnetic energy.

The main effect of the shear is the generation of strong ordered toroidal fields, $\langle B_y \rangle$. There is also a much weaker poloidal field component. The component in the latitudinal direction, $\langle B_x \rangle$, is about 10 times weaker and oriented mostly in the opposite direction, i.e. $\langle B_x \rangle \langle B_y \rangle < 0$ for most of the time. This is simply a consequence of the shear, $\partial U_y/\partial x < 0$, which turns a positive $\langle B_x \rangle$ into a negative $\langle B_y \rangle$.

2. Shear-driven accretion disc dynamos

A somewhat different situation is encountered in accretion discs, where there is no direct source of turbulence, because discs are hydrodynamically stable. Only in the presence of a magnetic field there is a linear instability (Velikhov 1959, Chandrasekhar 1960, 1961). This instability is now often called the magnetorotational or Balbus-Hawley (1991) instability. However, the flows generated by this instability would tend to destroy the magnetic field via turbulent diffusion. Nevertheless, at the same time the turbulence can also amplify the magnetic field via dynamo action. Simulations unanimously point towards the possibility of a cycle where the field generates turbulence and the turbulence generates more magnetic fields (Brandenburg et al. 1995, Hawley et al. 1996, Stone et al. 1996). In particular, in simulations of Brandenburg et al. (1995) there is a large scale magnetic field, which is oscillatory and varies on a time scale of about 30 orbits, $T_{\rm rot} = 2\pi/\Omega_0$, where Ω_0 is the angular velocity. Many quantities vary cyclically with the mean field, of which the toroidal component $\langle B_y \rangle$ is the strongest.

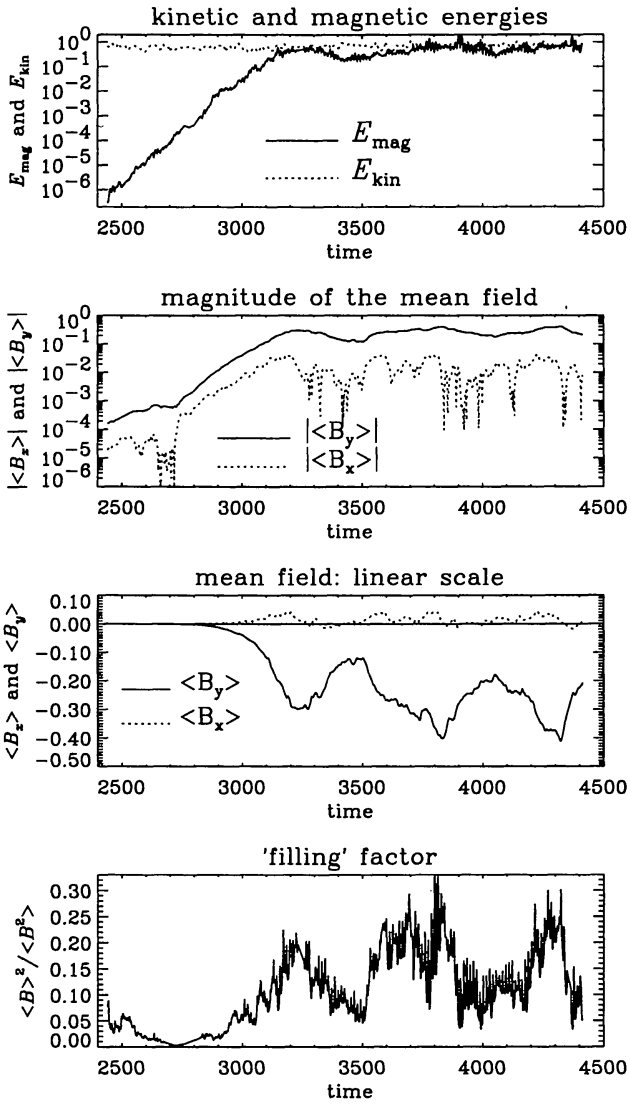

Figure 1. Evolution of magnetic and kinetic energies, mean magnetic field, and $\langle \boldsymbol{B} \rangle^2 / \langle \boldsymbol{B}^2 \rangle$ (which may be interpreted as a 'filling' factor) in a convection simulation with imposed shear.

In the case of the accretion disc simulations it is possible to estimate the magnitude and sign of the effective dynamo α parameter by correlating at different time steps the mean electromotive force with the resulting mean magnetic field and to establish a fit of the form $\langle \boldsymbol{u}' \times \boldsymbol{B}' \rangle_y = \alpha \langle B_y \rangle$ (Brandenburg et al. 1995, Brandenburg & Donner 1997). Here primes denote fluctuations. The α measured in that way is found to be *negative* in the upper disc plane. Therefore, the sign of α is in disagreement with that expected form kinetic and current helicities. The perhaps most convincing explanation for this negative sign is that the shear twists buoyant magnetic structures in the opposite sense as the Coriolis force (Brandenburg 1997, 1998).

The following calculation may shed some light on this question. It does reproduce the sign of $\alpha_{\rm dyn}$ that is seen in the simulations. It also yields a natural relationship between the two rather different quantities, the dynamo alpha $\alpha_{\rm dyn}$ and and the viscosity alpha parameter $\alpha_{\rm SS}$ used in accretion disc theory.

We assume that the vertical motions are governed by magnetic buoyancy, so

$$\frac{\partial u_z'}{\partial t} = -\frac{\rho'}{\rho} g = \frac{(B^2)'}{8\pi p} g \approx \frac{\langle B_y \rangle B_y'}{4\pi p} g, \tag{1}$$

where primes refer to deviations from some mean value, ρ is density, p is gas pressure, and g is gravity. We adopt a local cartesian coordinate system, where y corresponds to the azimuthal direction and x to the radial direction in cylindrical polar coordinates. The resulting electromotive force is then

$$\mathcal{E}_y = \langle u_z' B_x' - u_x' B_z' \rangle \approx \langle u_z' B_x' \rangle = +\langle B_y \rangle \frac{\langle B_x' B_y' \rangle}{4\pi p} g\tau, \tag{2}$$

where τ is some relevant time scale. Now, because of shear ($\partial u_y / \partial x < 0$) we have $\langle B_x' B_y' \rangle < 0$. The dynamo alpha quantifies the magnitude of the component of the electromotive force in the direction of the mean field. Therefore,

$$\mathcal{E}_y = \alpha_{\rm dyn} \langle B_y \rangle + ..., \tag{3}$$

and so we have (ignoring higher order terms)

$$\alpha_{\rm dyn} = +\frac{\langle B_x' B_y' \rangle}{4\pi p} g\tau. \tag{4}$$

In accretion disk theory the *negative* ratio of the horizontal Maxwell stress and the gas pressure is about twice the Shakura-Sunyaev viscosity parameter $\alpha_{\rm SS}$. Also, since $g = \Omega^2 z$, we can write

$$\alpha_{\rm dyn} \approx -2\alpha_{\rm SS} \Omega^2 z\tau \tag{5}$$

or, in terms of the inverse Rossby number $\mathrm{Ro}^{-1} = 2\Omega\tau$,

$$\frac{\alpha_{\rm dyn}}{\Omega H} \approx -\alpha_{\rm SS}\, \mathrm{Ro}^{-1} \frac{z}{H}. \tag{6}$$

The effects of rotation and shear are now hidden in the fact that the stress $\langle B_x' B_y' \rangle$ is negative, which is due to the negative shear. This estimate also

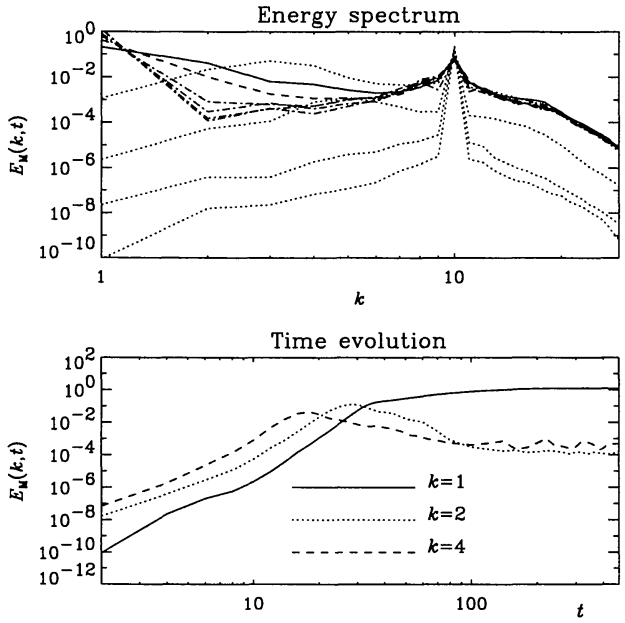

Figure 2. The inverse cascade seen in power spectra of the magnetic field taken at different times (upper panel). The four dotted curves are for $t = 2$, 4, 10, 20, the solid and dashed curves are for $t = 40$ and 60, respectively, and the dash-dotted curves are $t = 80$, 100, 200, and 400. The lower panel shows the evolution of the spectral power in the $k = 1$, 2, and 4 modes in a double-logarithmic plot.

assumes that the thermal expansion of buoyant tubes is small compared with the magnetic contraction due to the $\mathbf{B}\cdot\nabla\mathbf{B}$ term. Otherwise the sign may be the conventional one. In fact, the values of $\alpha_{\rm dyn}$ obtained from the above estimate are far too optimistic compared with the values obtained in the simulations. This suggests that $\alpha_{\rm dyn}$ is governed by some more delicate balance with other effects that tend to cancel each other. Thus, a proper analysis is called for. However, at present there is no other calculation that explains even the sign of $\alpha_{\rm dyn}$ that is seen in the simulations.

3. The inverse cascade effect in isotropically forced systems

Following the early work on inverse cascades (Pouquet et al. 1976) we now study a model where we adopt a *high* wavenumber forcing in the induction equation. Because the forcing is at high wavenumbers only ($k = 10$) the magnetic field evolution at the large scales ($k = 1$) is not immediately affected, except of course for the inverse cascade effect which governs the evolution on wavenumbers smaller than the forcing wavenumber. We also point out that the general behavior is similar, regardless of whether the forcing is applied in the induction equation or in the momentum equation.

Looking at power spectra of the magnetic field at subsequent times (figure 2) we see that the energy at the largest possible scale in the system ($k = 1$) grows

until some saturation level is reached at around $t = 40$; see the lower panel of figure 2. Curiously enough, at the time when the $k = 1$ mode reaches saturation the power in the $k = 2$ mode begins to be suppressed (see the dotted line). Looking more carefully at this plot reveals that at the time when the $k = 2$ mode began to saturate (at around $t = 20 - 30$) the power in the next higher modes, $k = 3$ and $k = 4$, was suppressed. This has also been observed in similar calculations of low Reynolds number flows (Gilbert & Sulem 1990, Galanti et al. 1991, Galanti & Sulem 1991). In our case the Reynolds numbers (ordinary and magnetic), based on the box size and the rms velocity, are around 140. However, the Reynolds number based on the wavenumber 10 is only 14. In that sense our simulation too is rather diffusive.

The orientation of the magnetic field is not determined a priori and depends on chance and on initial conditions. Sometimes we found a field that varied mostly in the x-direction, while for other simulations the field varied mostly in the y or z-directions. If the mean field varies only in the x-direction, for example, then $\partial_y \langle \boldsymbol{B} \rangle = \partial_z \langle \boldsymbol{B} \rangle = 0$ and only $\partial_x \langle \boldsymbol{B} \rangle$ is nontrivial. Then, however, because

$$0 = \boldsymbol{\nabla} \cdot \langle \boldsymbol{B} \rangle = \partial_x \langle B_x \rangle, \tag{7}$$

we have $\langle B_x \rangle = \text{const} = 0$, so $\langle \boldsymbol{B} \rangle = (0, \langle B_y \rangle, \langle B_z \rangle)$. In other words, the field vector lies in a plane whose normal is parallel to the direction in which it varies, but it has no component in that direction. Once the large scale field has selected a preferred direction, it will stick to it for all times. We note, however, that we never encountered a case where the field is oblique to any of the coordinate planes. An oblique mean field would diffuse faster, because the turbulent diffusion operator, $\eta_t(k_x^2 + k_y^2) = 2\eta_t k_{\rm min}^2$, is always larger than just $\eta k_x^2 = \eta_t k_{\rm min}^2$. This is probably the reason why diagonal fields are not being generated.

In figure 3 we show the resulting mean magnetic field from a simulation in which the preferred direction of the mean field is the z-direction. Note that there is a 90° phase difference between the x and y-components of the mean magnetic field.

The approach just described allows us to study the evolution and saturation of the large scale magnetic field. An obvious question is then whether the field produced by the inverse cascade resembles qualitatively and perhaps even quantitatively the field generated by an α^2 dynamo, and if so, what are then the corresponding values of α and turbulent diffusivity, η_t.

4. Connection with an alpha-squared dynamo

The mean magnetic field found in the previous section resembles in many ways an α^2 dynamo. In such a dynamo the large scale field is governed by the equations

$$\frac{\partial \langle B_x \rangle}{\partial t} = -\alpha \frac{\partial \langle B_y \rangle}{\partial z} + (\eta + \eta_t) \frac{\partial^2 \langle B_x \rangle}{\partial z^2}, \tag{8}$$

$$\frac{\partial \langle B_y \rangle}{\partial t} = +\alpha \frac{\partial \langle B_x \rangle}{\partial z} + (\eta + \eta_t) \frac{\partial^2 \langle B_y \rangle}{\partial z^2}, \tag{9}$$

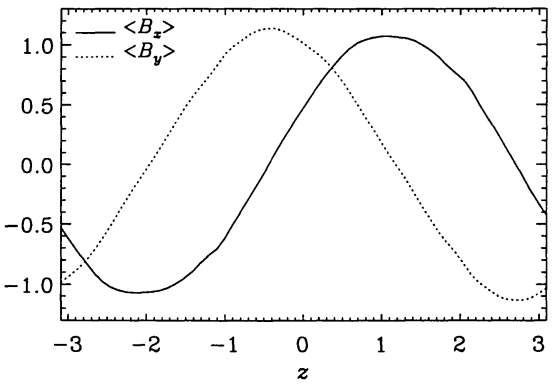

Figure 3. The mean magnetic field components, $\langle B_x \rangle$ and $\langle B_y \rangle$, as functions of z in a simulation where the mean field varies only in the z-direction.

where we have assumed that the mean field varies only in the z-direction, which is the situation in the particular solution displayed in figure 3 (section 3.). The averages are taken over the x and y directions. In the saturated case the field is dominated by the smallest waver number $k = 1$; see the inset of figure 2. Therefore we now take the solution to be of the form

$$\langle B_x \rangle = \hat{B}_x(t) \sin(z - z_0), \quad \langle B_y \rangle = \hat{B}_y(t) \cos(z - z_0), \tag{10}$$

where z_0 is a constant (phase factor). With this, Eqs. (8) and (9) take the form

$$\frac{\partial \hat{B}_x}{\partial t} = \alpha \hat{B}_y - (\eta + \eta_t)\hat{B}_x, \tag{11}$$

$$\frac{\partial \hat{B}_y}{\partial t} = \alpha \hat{B}_x - (\eta + \eta_t)\hat{B}_y. \tag{12}$$

In the steady state we have $\alpha = \eta + \eta_t$. In order to estimate the value of α we modify the actual field in the simulation by setting momentarily the mean field in either the x or the y-direction to zero, i.e. we replace at some instance in time $B_x \to B_x - \langle B_x \rangle$ or $B_y \to B_y - \langle B_y \rangle$. Looking at eq. (11) we see that setting $\langle B_x \rangle = \hat{B}_x = 0$ means that immediately after this manipulation the $\hat{B}_x$ field should recover at a rate $\alpha \hat{B}_y$. This rate is approximately 0.02 (see figure 4), and since $\hat{B}_y \approx 1$ we have $\alpha \approx 0.02$. This value is already affected by the nonlinear feedback in the system (alpha-quenching, for example). Assuming that the value of α is the same before and after removing one of the two mean field components we have therefore $\eta + \eta_t \approx \alpha \approx 0.02$. Since in this simulation $\eta = 0.01$ we have $\eta_t \approx \eta$. Those values of α and η_t are rather small, suggesting again that the effective magnetic Reynolds number is small.

This method can in principle be applied to systems with different field strengths, different magnetic Reynolds numbers, and different amounts of helicity.

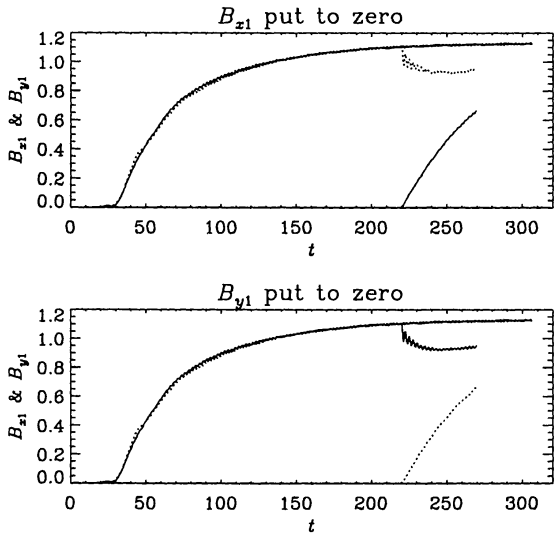

Figure 4. Response of the large scale field after removing the mean field from the B_x and B_y fields, respectively. After $t = 220$ the field component that was set to zero ($\hat{B}_x$ in the upper panel, $\hat{B}_y$ in the lower) began to grow at a rate ≈ 0.02.

5. Conclusions

In this paper we have highlighted some important issues that have arisen recently in connection with understanding dynamos in stars and other astrophysical bodies. In all cases studied so far a large scale magnetic field can be generated whose strength approaches the equipartion field strength. The main limitation so far remains the fact that the magnetic Reynolds numbers do not exceed a few hundred. Nevertheless, the flows are fairly turbulent and provide already now an excellent opportunity to study details of the dynamo process that were previously possible only in connection with rather simple mean-field type models.

References

Balbus, S. A. & Hawley, J. F. 1991 A powerful local shear instability in weakly magnetized disks. I. Linear analysis. *Astrophys. J.* 376, 214-222.

Brandenburg, A. 1997 Large scale turbulent dynamos. *Acta Astron. Geophys. Univ. Comenianae* XIX, 235-261.

Brandenburg, A. 1998 Theoretical Basis of Stellar Activity Cycles. In *Tenth Cambridge Workshop on Cool Stars, Stellar Systems, and the Sun* (ed. R. Donahue & J. Bookbinder), pp. 173-191. Astron. Soc. Pac. Conf. Ser., Col. 154.

Brandenburg, A. & Donner, K. J. 1997 The dependence of the dynamo alpha on vorticity. *Monthly Notices Roy. Astron. Soc.* 288, L29-L33.

Brandenburg, A., Nordlund, Å., Stein, R. F., & Torkelsson, U. 1995 Dynamo generated turbulence and large scale magnetic fields in a Keplerian shear flow. *Astrophys. J.* 446, 741-754.

Brandenburg, A., Jennings, R. L., Nordlund, Å., Rieutord, M., Stein, R. F., & Tuominen, I. 1996 Magnetic structures in a dynamo simulation. *J. Fluid Mech.* 306, 325-352.

Brandenburg, A., Nordlund, Å., & Stein, R. F. 1999 "Simulation of a convective dynamo with imposed shear," *Astron. Astrophys.* (to be submitted).

Chandrasekhar, S. 1960 The stability of non-dissipative Couette flow in hydromagnetics. *Proc. Natl. Acad. Sci.* 46, 253-257.

Chandrasekhar, S. 1961 *Hydrodynamic and Hydromagnetic Stability.* Dover Publications, New York., pp. 384

Galanti, B. & Sulem, P.-L. 1991 Inverse cascades in three-dimensional anisotropic flows lacking parity invariance. *Phys. Fluids* A 3, 1778-1784.

Galanti, B., Sulem, P.-L. & Gilbert, A. D. 1991 Inverse cascades and time-dependent dynamos in MHD flows. *Physica* D 47, 416-426.

Gilbert, A. D. & Sulem, P.-L. 1990 On inverse cascades in alpha effect dynamos. *Geophys. Astrophys. Fluid Dyn.* 51, 243-261.

Hawley, J. F., Gammie, C. F., & Balbus, S. A. 1995 Local three-dimensional magnetohydrodynamic simulations of accretion discs. *Astrophys. J.* 440, 742-763.

Hawley, J. F., Gammie, C. F., & Balbus, S. A. 1996 Local three dimensional simulations of an accretion disk hydromagnetic dynamo. *Astrophys. J.* 464, 690-703.

Nordlund, Å., Brandenburg, A., Jennings, R. L., Rieutord, M., Ruokolainen, J., Stein, R. F., & Tuominen, I. 1992 Dynamo action in stratified convection with overshoot. *Astrophys. J.* 392, 647-652.

Pouquet, A., Frisch, U., & Léorat, J. 1976 Strong MHD helical turbulence and the nonlinear dynamo effect. *J. Fluid Mech.* 77, 321-354.

Stone, J. M., Hawley, J. F., Gammie, C. F., & Balbus, S. A. 1996 Three dimensional magnetohydrodynamical simulations of vertically stratified accretion disks. *Astrophys. J.* 463, 656-669.

Velikhov, E. P. 1959 Stability of an ideally conducting liquid flowing between cylinders rotating in a magnetic field. *Sov. Phys. JETP* 36, 1398-1404. (Vol. 9, p. 995 in English translation)